Theory of radiative shocks in the mixed, optically thick-thin case

Ryan G. McClarren,[1,a)] R. Paul Drake,[2] J. E. Morel,[1] and James Paul Holloway[3]
[1]*Department of Nuclear Engineering, Texas A&M University, College Station, Texas 77843-3133, USA*
[2]*Space Physics Research Laboratory, Atmospheric Oceanic and Space Sciences, University of Michigan, Ann Arbor, Michigan 48109, USA*
[3]*Department of Nuclear Engineering and Radiological Science, University of Michigan, Ann Arbor, Michigan 48109, USA*

A theory of radiating shocks that are optically thick in the downstream (postshock) state and optically thin in the upstream (preshock) state, which are called thick-thin shocks, is presented. Relations for the final temperature and compression, as well as the postshock temperature and compression as a function of the shock strength and initial pressure, are derived. The model assumes that there is no radiation returning to the shock from the upstream state. Also, it is found that the maximum compression in the shock scales as the shock strength to the 1/4 power. Shock profiles for the material downstream of the shock are computed by solving the fluid and radiation equations exactly in the limit of no radiation returning to the shock. These profiles confirm the validity and usefulness of the model in that limit. © *2010 American Institute of Physics*.
[doi:10.1063/1.3466852]

I. INTRODUCTION

Radiative shocks are one of the fundamental types of behavior that arise within radiation-hydrodynamic systems. In order to accurately describe radiation-hydrodynamic systems, one must consider both the dynamic behavior of the matter and of the radiation. Radiation hydrodynamic behavior in general includes radiation-modified oscillating waves, nonlinear radiative heat waves and ionization fronts, and radiative shocks. All these systems more often than not arise in plasmas, as radiation intense enough to carry significant energy is typically ionizing radiation. Many such systems are also high-energy-density systems. It is no surprise that the available monographs that cover radiation hydrodynamics[1–4] all treat radiative shocks.

Radiative shocks can be characterized in two fundamental ways. The first deals with the mechanism through which radiation influences the system. The so-called flux-dominated regime has a flux of radiation energy that is nonnegligible when compared with the flux of material energy. As temperatures in the system increase, the radiation pressure, which is a factor $1/c$ smaller than the radiation flux, can become comparable to or exceed the material pressure in the pressure-dominated regime. The flux-dominated regime is more readily accessible in the laboratory and has been the topic of several previous theoretical studies.[1–3,5,6] The relation between the flux-dominated and pressure dominated regimes has recently been addressed by Michaut *et al.*[7]

Within the context of flux-dominated radiative shocks, the anticipated shock structure depends essentially on the optical depth of the upstream and downstream media, which provides the second way to characterize these shocks.[8] Optical depth refers to the spectrally weighted mean of the number of mean-free paths for the thermal radiation. A region is said to be optically thick when its optical depth is large and optically thin when the optical depth is small. In other words, an optically thick region is opaque to radiation, whereas an optically thin region is transparent to radiation. It is possible to classify shocks with a two-word designation with the optical thickness of the downstream medium, followed by the optical thickness of the upstream medium. For example, the case dealt with in this paper has the downstream region optically thick and the upstream optically thin, so one can call this a thick-thin radiative shock.

Previous work on radiative shocks, besides focusing on the flux-dominated regime, has dealt mainly with the thick-thick and thin-thin cases. The classic monograph of Zel'dovich and Raizer[1] deals with the thick-thick case as have several other researchers[2–6,9,10] recently, in addition, there are a number of early papers cited by Mihalas and Weibel-Mihalas.[2] In this case radiation energy from the downstream state heats the upstream material, forming what is known as a precursor. This acts as a mechanism to return radiative energy to the shock. Due to the fact that the shock cannot lose energy radiatively, the maximum compression of a thick-thick shock is the same as for a nonradiative shock. At the other extreme, the theory of the thin-thin case has been investigated by Chevalier and Imamura[11] and is detailed in several books.[3,12] The thin-thin case has all of the energy leave the system and higher compression can be reached.

On the other hand, the only study of the theory of thick-thin shocks can be found in Drake's monograph.[3] That description of thick-thin shocks relied on several, reasonable, simplifying assumptions. This work dispenses with those simplifications to produce a detailed theory of thick-thin shocks that ultimately justifies the previous simplifying assumptions in the correct limits. Besides this theoretical work, computational results for a thick-thin shock were provided by Winkler, Norman, and Mihalas.[13] With the benefit of
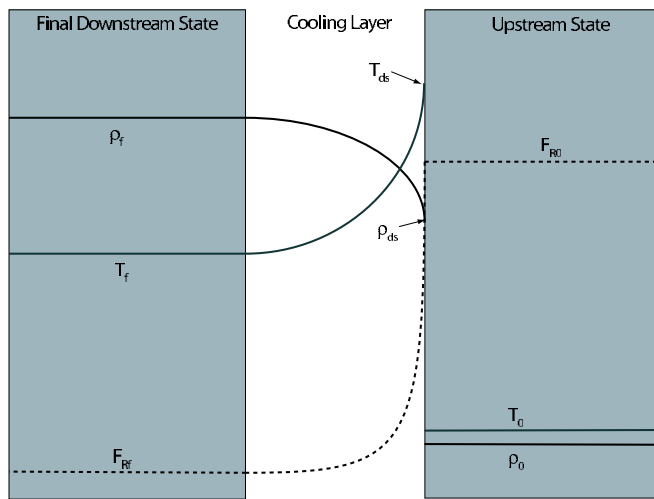
---

a)Electronic mail: rgm@tamu.edu.

FIG. 1. (Color online) Cartoon of the three-layer model, the shock is moving left to right with speed u_s. The density jump is at the boundary between the upstream state and the cooling layer. Note that in this three-layer model the radiation flux is constant in the upstream portion of the shock.

hindsight, one can observe several of the phenomenon of thick-thin shocks that are identified in this paper in their well resolved simulations. In addition, some simulations of recent laboratory experiments have produced results for thick-thin shocks.[14–16] However, none of these papers have considered the theory of thick-thin shocks as such and some of them have failed to carefully consider the fact that the radiation energy density is much lower in systems that are not optically thick than in systems that are optically thick. Overall, the lack of study of the thick-thin case is surprising in that this sort of radiative shock is accessible in laboratory experiments. This is the case because the upstream medium is finite in an experiment and the experiment is of limited duration. The radiation in most experiments either is used up ionizing the upstream material or in some measure escapes in the upstream direction. In either event, the corresponding radiative energy does not return to the shock as it would if the upstream material were optically thick.

To model thick-thin shocks a three layer model that accounts for the upstream region, a cooling layer just behind the density jump, and a final downstream region is used. This model is diagrammed in Fig. 1.

The upstream region has constant values for the radiation flux as well as density and temperature. The density jump is between the cooling layer and the upstream region. The cooling layer contains the maximum temperature in the problem and that temperature cools via radiation until the final downstream state. A salient feature of this cooling layer is that radiative transfer in this layer cannot in general be well treated using the Eddington approximation as part of a diffusive model because there can be places where the flow of radiation energy is uphill in the sense that the flux of radiation is in the same direction as the gradient of the energy density.[17] Using a diffusive model for radiative transfer in the cooling layer leads to a monotonic behavior of the radiation energy in the cooling layer.[2,4,9,10] Also in this model, the radiation flux in the upstream region is a result of

radiation energy flowing from the downstream state and the cooling layer into the upstream region. All of the radiation that flows into the upstream state from the downstream state does not return to the shock.

In the three-layer model the radiation flux at the final downstream state is zero. This is consistent with the assumptions in the optically thick shock case. The upstream material, however, has a finite radiation flux that is equal to the right-moving radiation flux at the density jump. A finite upstream radiation flux differs from the optically thick case where far upstream the radiation flux is also assumed to be zero. Moreover, the assumption that radiation does not interact with the thin upstream material eliminates the precursor found in an optically thick shock.

The three-layer model is valid after the shock has attained a steady profile. In an experiment the transient leading to the steady profile would have a Marshak-like radiation wave traveling through the upstream region until a constant temperature was achieved. It is at this point that the steady profile would emerge. The three-layer model does not incorporate the adaptation zone on the downstream boundary of the cooling layer. In this adaptation zone the density, temperature, and radiation flux transition from the rapidly varying profile of the cooling layer to the constant solution in upstream and downstream regions. By ignoring this adaptation zone, these solutions also ignore their (small) effect.

The effect of the adaptation zone is included in the shock profiles computed below. These profiles are found by integrating the fluid dynamics equations with a postulated form of the radiation mean intensity and then iterating on this mean intensity until convergence. The results of these profile calculations demonstrate that the three-layer model is a useful description of the energy balance and structure of a thick-thin shock.

Below relations for the state variables in the downstream region using an exact treatment of the fluid dynamics and the radiative transfer are derived. This is followed by a discussion of a threshold shock strength above which the final temperature is below the initial temperature and a simple scaling law to predict the final compression in the shock is given. Then radiative transfer in the shocked material in the three-layer model is discussed. Finally, shock profiles for a model including the adaptation zone are presented before concluding.

II. MODEL SPECIFICATION

It is assumed that the plasma is in a regime where it can be described by fluid equations. Also, this model assumes that the ion and electron temperatures can be characterized by a single temperature, T. For the equations that govern the continuity and momentum of the hydrodynamic variables, consider the standard Euler equations for planar geometry,

$$\frac{\partial \rho}{\partial t} + \frac{\partial}{\partial x}(\rho u) = 0, \tag{1a}$$

$$\frac{\partial}{\partial t}(\rho u) + \frac{\partial}{\partial x}(\rho u^2 + p) = 0. \tag{1b}$$

The conservation of energy is expressed as

$$\frac{\partial}{\partial t}(\rho E + E_r) + \frac{\partial}{\partial x}[v(\rho E + p) + F_r] = 0, \tag{1c}$$

where ρ is the density, u is the material velocity, and p is the pressure; the radiation energy is denoted by E_r and the radiation flux is F_r. The total material energy density is given by $E = \frac{1}{2}\rho u^2 + \rho e$. Furthermore, this model assumes the material can be treated as a polyatomic gas governed by a γ law equation of state. This gives the internal energy density as $e = p/(\gamma - 1)$. Equation (1) is valid in the flux-dominated regime,[3] where the radiation pressure is small compared to the hydrodynamic pressure. If the radiation pressure was not small, then the governing equations would become much more complicated.[18]

The radiation flux is given by taking the first moment of the spectrally integrated specific intensity I,

$$F_r(x,t) = 2\pi \int_{-1}^{1} d\mu\, \mu I(x,\mu,t),$$

where μ is the cosine of the angle between the x-axis and the direction of radiation propagation. The sign convention will be such that flux of radiation moving upstream (to the right in Fig. 1) is positive, and the flux of radiation moving downstream (to the left in Fig. 1) is negative. The specific intensity is governed by the steady radiative transfer equation[5,12]

$$\mu \frac{\partial I}{\partial x} = \kappa(B - I), \tag{2}$$

where the Planck-averaged absorption opacity is denoted by $\kappa(x)$. In this study one finds the integral form of Eq. (2) to be most useful. This equation can be found by integrating Eq. (2) along photon trajectories to get the integral radiative transfer equation

$$I(x,\mu) = \begin{cases} I(x_R)e^{\int_x^{x_R} dx'\, \kappa(x')/|\mu|} + \displaystyle\int_x^{x_R} dx'\, \frac{\kappa(x')B(x')}{|\mu|}e^{\int_x^{x'} dx'\, \kappa(x')/|\mu|}, & \mu < 0 \\[2ex] I(x_L)e^{\int_{x_L}^{x} dx'\, \kappa(x')/\mu} + \displaystyle\int_{x_L}^{x} dx'\, \frac{\kappa(x')B(x')}{\mu}e^{\int_{x'}^{x} dx'\, \kappa(x')/\mu}, & \mu > 0 \end{cases} \tag{3}$$

for the region $x \in [x_L, x_R]$, where x_L and x_R are the left and right system boundaries, respectively. The integral radiative transfer equation will assume a much simpler form later in this work when written in terms of optical depth of a given layer

$$\tau = \int_a^b dx\, \kappa(x), \tag{4}$$

with a and b as the left and right boundaries of the layer.

Here, the radiative transfer model ignores scattering, a reasonable approximation in the regime of interest because the magnitude of energy exchange for absorption is larger than that for Thomson scattering, and the temperatures are low enough that Compton scattering is negligible. The function $B(x) \equiv B[\mu, T(x)]$ is the spectrally integrated Planck function

$$B[\mu, T(x)] = \frac{\sigma_{SB} T^4(x)}{\pi},$$

with σ_{SB} as the Stefan–Boltzmann constant. Note that the flux of radiation in the positive x-direction is given by

$$\begin{aligned} F_r^+ &= 2\pi \int_0^1 d\mu\, \mu I \\ &= 2\pi I(x_L) E_3\left[\int_{x_L}^x dx'\, \kappa(x')\right] \\ &\quad + 2\pi \int_{x_L}^x dx'\, \kappa(x') B(x') E_2\left[\int_{x'}^x dx''\, \kappa(x'')\right], \end{aligned} \tag{5}$$

where $E_n(x)$ is the exponential integral function of order n. The flux in the negative x-direction is

$$\begin{aligned} F_r^- &= 2\pi \int_{-1}^0 d\mu\, \mu I \\ &= -2\pi I(x_R) E_3\left[\int_x^{x_R} dx'\, \kappa(x')\right] \\ &\quad - 2\pi \int_x^{x_R} dx'\, \kappa(x') B(x') E_2\left[\int_x^{x'} dx''\, \kappa(x'')\right]. \end{aligned} \tag{6}$$

From these definitions, the flux from a material in equilibrium, i.e., $I = B(\mu, T)$, has the properties

$$F_r = 2\pi B \int_{-1}^1 d\mu\, \mu = 0$$

and

$$F_r^+ = - F_r^- = \sigma_{SB} T^4.$$

The half-range fluxes $F_r^\pm$ will be important in treating the radiative transfer of the shock profile.

Below the shock will be modeled with a three-layer model that includes the initial (upstream) state, a cooling layer just behind the density jump, and the final downstream state. The upstream state is considered to be optically thin to such a degree that interaction between the radiation and the material is negligible. A salient feature of this model is that any radiation traveling into the upstream region cannot return to the shock.

This model does not include the adaptation zone between the cooling layer and the final downstream state. In the adaptation zone the radiation intensity becomes isotropic over several optical depths. As the radiation slowly approaches an isotropic distribution, the material temperature and density approach their final values. This effect is relatively small because the main mechanism for coupling the radiation to the material is through the radiation mean intensity, which is proportional to the zeroth angular moment of the intensity. One can ignore the effects of the adaptation zone when concerned about calculating the energy balance of the shock. Nevertheless, this region affects the detailed shock profile and its effect is included when computing the shock profile below.

III. CONSERVATION RELATIONS

Now consider the model equations in a steady frame where the upstream material flows into the shock with velocity $-u_s$. Denoting quantities evaluated at the upstream conditions with the subscript "0," the following relations hold for the flux of mass, momentum, and energy throughout the shock profile:

- Conservation of mass flux:

$$\rho u = - \rho_0 u_s. \tag{7a}$$

- Conservation of momentum flux:

$$\rho u^2 + p = - (\rho_0 u_s) u + p = \rho_0 u_s^2 + p_0. \tag{7b}$$

- Conservation of energy flux:

$$F_r + \frac{\gamma}{\gamma - 1} pu + \frac{\rho u^3}{2} = - \frac{\rho_0 u_s^3}{2} - \frac{\gamma}{\gamma - 1} p_0 u_s + F_{r0}. \tag{7c}$$

The relations in Eq. (7) are derived by integrating Eq. (1)

in a steady frame from the upstream state to the a generic point.

If one introduces the inverse compression $\eta = \rho_0 / \rho$, the normalized radiation flux $F_{rn} = 2F_r / (\rho_0 u_s^3)$, and the normalized pressure

$$p_n = \frac{p}{\rho_0 u_s^2} = (1 - \eta) + p_{0n}, \tag{8}$$

Equation (7) can be combined into a single equation,

$$F_{rn} - F_{rn0} = - 1 + \frac{2\gamma}{\gamma - 1} [\eta - p_{0n}(1 - \eta)] - \frac{\gamma + 1}{\gamma - 1} \eta^2. \tag{9}$$

From Eq. (9) one can find the value of η at any point in the system, provided F_{rn} is known.

A. The final state

The final value of the inverse compression can be found by noting that the final radiation flux is zero and using the quadratic formula on Eq. (9) to get

$$\eta_f = \frac{\gamma(1 + p_{0n}) - \sqrt{(p_{0n}\gamma - 1)^2 + F_{rn0}(\gamma^2 - 1)}}{\gamma + 1}. \tag{10}$$

In the case of $F_{rn0} = 0$ the value of η_f recovers the value for the thick-thick case.[6] The quantities u and T can also be related to η. Using the gas "constant,"

$$R = \frac{k_B(Z + 1)}{A m_p},$$

for a gas ionized Z times with atomic weight A and with k_B and m_p denoting the Boltzmann constant and the mass of a proton, respectively, it is possible to write the specific pressure, $RT = p/\rho$, in dimensionless form as

$$RT_n = \frac{RT}{u_s^2} = \eta(1 - \eta) + p_{0n}\eta. \tag{11}$$

Using the value of η_f the final value of RT_n is

$$RT_{nf} = \frac{[p_{0n}\gamma + \gamma - \sqrt{(p_{0n}\gamma - 1)^2 + F_{rn0}(\gamma^2 - 1)}][p_{0n} + \sqrt{(p_{0n}\gamma - 1)^2 + F_{rn0}(\gamma^2 - 1)} + 1]}{(\gamma + 1)^2}. \tag{12}$$

This derivation has yet to determine the value of F_{rn0}, in the model this is the right-moving radiation flux at the density jump. This flux is required to find the state, however, as shown below in the analysis of the cooling layer, F_{rn0} is a function of the temperature at the final state.

B. The immediate postshock state

The value of the inverse compression just after the density jump can be easily found by noting that at this point $F_{rn}=F_{rn0}$ and solving Eq. (9) to get

$$\eta_{ds} = \frac{\gamma-1}{\gamma+1} + \frac{2\gamma}{\gamma+1}p_{0n}. \tag{13}$$

The value of η_{ds} for the thick-thin shock is the value of the *final* downstream inverse compression for the optically thick case. In other words, in the final downstream state for an optically thick shock the difference between the local radiation flux and the far upstream radiation flux is zero; this is the case at the density jump for the thick-thin shock. It is at the density jump that $F_{r0}=F_r$, making the right-hand side of Eq. (9) zero. The thick-thin shock then goes on to compress further until it reaches the final state.

Using Eq. (13) one can also find the maximum value for the temperature at the downstream state by substituting the value of η_{ds} into Eq. (11) to get

$$RT_{dsn} = \frac{(2-(\gamma-1)p_0)(2\gamma p_0 + \gamma-1)}{(\gamma+1)^2}. \tag{14}$$

The temperature in Eq. (14) is also the value for the final downstream temperature in the optically thick case. Therefore, the maximum downstream temperature in the thick-thin case is less than the maximum downstream temperature in the optically thick case.

C. The cooling layer

At the edge of the final downstream state the net radiation flux is zero because the final state is defined as the state where the radiation flux is zero. Given that the final temperature state is characterized by a single temperature, there is zero net radiation flux inside the region. Nevertheless, at the boundary between the final state and the cooling layer there is a right-moving radiation flux from the final state, $\sigma_{SB}T_f^4$. This right-moving flux from the final state balances the total left-moving radiation flux from the cooling layer, $-F_{cl}$,

$$\sigma_{SB}T_f^4 - F_{cl} = 0. \tag{15}$$

In addition to this equation, an effective temperature T_{eff} can be used to model the emission source of the cooling layer. This as yet unspecified effective temperature has the effect of making the flux from the cooling layer at the density jump, the right edge of the cooling layer, an equal and opposite contribution to the left-moving flux at the edge of the cooling

layer. Thereby, the contribution to the right-moving flux at the density jump from the cooling layer is F_{cl}. This approximation will be justified later by detailed calculations where this assumption is not made and the resulting final state compression/temperatures are not affected. In addition to F_{cl}, at the density jump there will be a contribution to the right-moving radiation flux from the final downstream state. This contribution can be calculated by taking the known intensity at the edge of the final state and using the integral transport equation to calculate the flux at the right edge of the cooling layer,

$$2\pi\int_0^1 d\mu\mu\frac{\sigma_{SB}T_f^4}{\pi}e^{-\tau_{cl}/\mu}$$

$$= 2\sigma_{SB}T_f^4 E_3(\tau_{cl}) \approx (1-2\tau_{cl})\sigma_{SB}T_f^4 + O(\tau_{cl}^2),$$

where τ_{cl} is the optical depth of the cooling layer, assumed to be small. There is no left moving radiation flux at the density jump because no radiation is moving leftward from the upstream state. Therefore conservation of radiation flux at the density jump gives

$$F_{rn0} = \frac{2\sigma_{SB}T_f^4 E_3(\tau_{cl}) + F_{cl}}{\frac{1}{2}\rho_0 u_s^3}$$

$$= \frac{1+2E_3(\tau_{cl})}{\frac{1}{2}\rho_0 u_s^3}\sigma_{SB}T_f^4 = Q[1+2E_3(\tau_{cl})](RT_{fn})^4, \tag{16}$$

where $E_3(x)$ is the exponential integral function of order 3. In this expression Q is the dimensionless shock strength defined by Drake for the theory of optically thick radiating shocks,[5,6]

$$Q = \frac{2\sigma_{SB}u_s^5}{R^4\rho_0}. \tag{17}$$

Under the assumption that τ_{cl} is small, the expansion of Eq. (16) gives

$$F_{rn0} = 2Q(1-\tau_{cl})(RT_{fn})^4 + O(\tau_{cl}^2). \tag{18}$$

The result in Eq. (18) gives that the radiation flux traveling upstream from the density jump is, to leading order, twice the radiation flux moving rightward from the final state. The approximation that F_{r0} is twice $\sigma_{SB}T_f^4$ was originally mentioned by Drake,[3] but here the accuracy of that approximation is shown to be $O(\tau_{cl})$.

Under the approximation that the cooling layer is small, an assumption justified below, one can write F_{rn0} as

$$F_{rn0} = 2Q[\eta_f(1+p_{0n}-\eta_f)]^4, \tag{19}$$

then, to leading order in τ_{cl}, Eq. (10) becomes

$$\eta_f = \frac{\gamma(1+p_{0n}) - \sqrt{(p_{0n}\gamma-1)^2 + 2Q[\eta_f(1+p_{0n}-\eta_f)]^4(\gamma^2-1)}}{\gamma+1}. \tag{20}$$

This is a quartic equation that is solved numerically to find the final inverse compression. The inverse compression then allows us to compute the final temperature through Eq. (11).
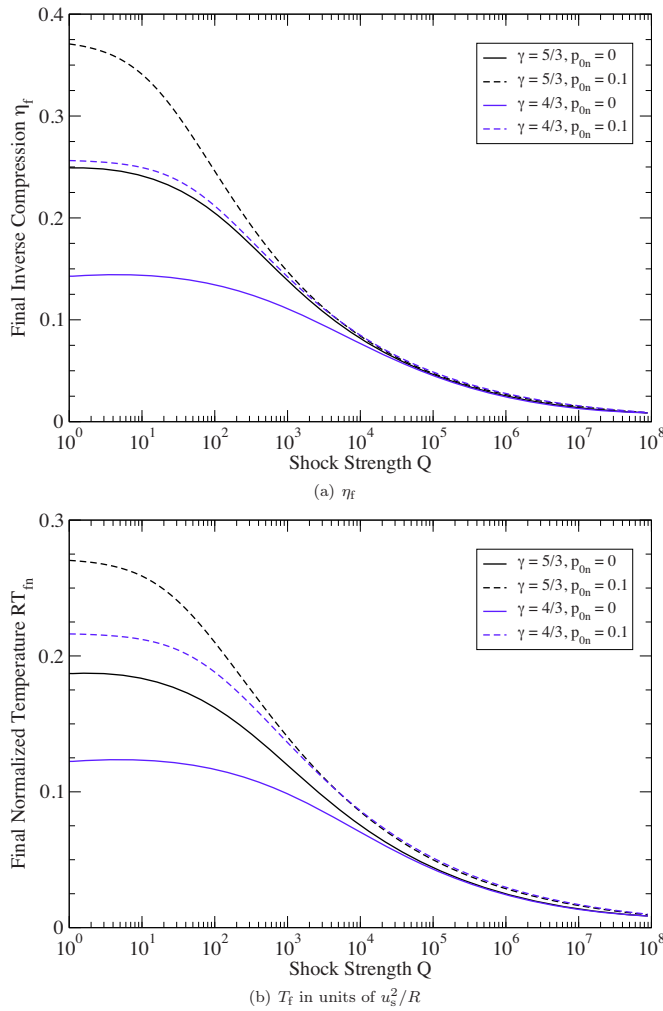
(a) η_f

(b) T_f in units of u_s^2/R

FIG. 2. (Color online) Final downstream values of the inverse compression and temperature as function of Q.

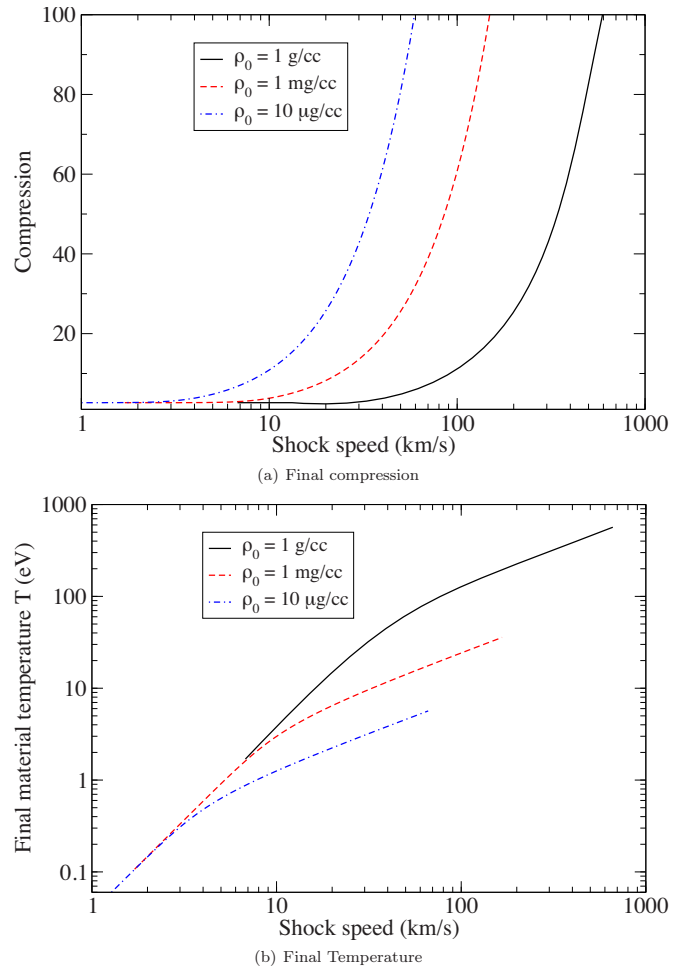(a) Final compression

(b) Final Temperature

FIG. 3. (Color online) Final downstream values of the compression and temperature as a function of shock speed for xenon with $Z=9$, $\gamma=5/3$, and $p_{0n}=0.1$ and several initial densities.

In Fig. 2 the values for the final inverse compression and temperature are plotted as a function of the shock strength. In the figure note that the final inverse compression goes to zero (that is, the compression goes to infinity) as the shock strength goes to infinity. Similarly, the specific pressure, RT_{fn}, limits to zero as the shock strength increases to infinity. Though RT_{fn} goes to zero, the value of the final temperature does not go to zero because the temperature is proportional to $Q^{2/5}RT_n$. This can be seen in the example below.

To demonstrate the final temperatures and compression in a specific case, consider the shock to be occurring in xenon gas with $Z=9$, $A=130$, $p_{0n}=0.1$, $\gamma=5/3$, and three different initial densities. In Fig. 3 one can see how the final state of the material is affected by the initial density as a function of the shock speed: shocks propagating into lower initial densities lead to higher compressions and lower temperatures than with higher upstream densities.

D. The thickness of the cooling layer

Above we were able to compute the final inverse compression and temperature under the assumption that the thickness of the cooling layer τ_{cl} is small. In this section we will verify that the results from the three-layer model are consistent in that assumption. As we will discuss below, in a three-layer model τ_{cl} can be interpreted as the effective width over which the material radiates at the effective temperature. Provided we know the profile of the temperature as a function of τ, we can compute the thickness of the cooling layer using the integral radiative transfer equation to find F_{cl}. It turns out that this flux is, to second order in τ_{cl}, a linear function of τ_{cl}. Using this computed value of F_{cl} and the equation for the net flux at the boundary between the cooling layer and the final state, Eq. (15), we arrive at a value for τ_{cl}. The value of τ_{cl} computed below will confirm that the optical thickness of the cooling layer is indeed small.

The left-moving flux at the boundary between the cooling layer and the final state is given by the formula

$$F_{cl} = -F_r^-(\tau_{cl}) = 2\pi \int_{-1}^0 d\mu \int_0^{\tau_{cl}} d\tau f(\tau) e^{-(\tau_{cl}-\tau)/|\mu|}$$

$$= \int_0^{\tau_{cl}} d\tau f(\tau) E_2(\tau_{cl}-\tau), \qquad (21)$$

where $f(\tau)$ is the emission source inside the cooling layer with τ the distance from the density jump in mean-free paths and $E_2(x)$ is the exponential integral function of order 2.
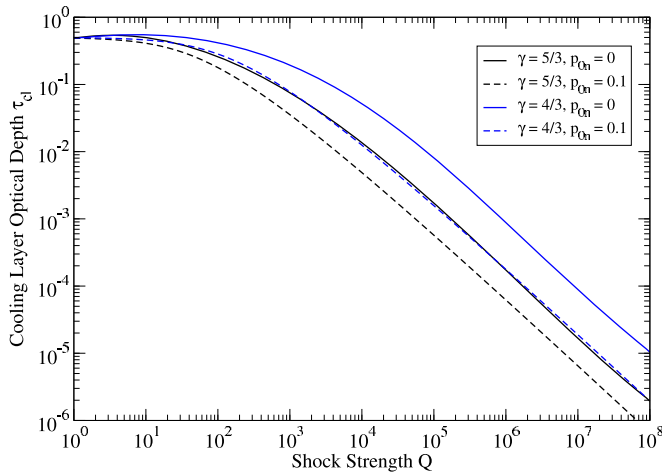
FIG. 4. (Color online) Values of the optical thickness of the cooling layer as function of Q shown on a semilog scale. The $\gamma=4/3$, $p_{0n}=0.1$, and $\gamma=5/3$, $p_{0n}=0$ lines are coincident on the plot.

Also, $f(0)=B(T_{ds})$ and $f(\tau_{cl})=B(T_f)$. Upon expanding $f(\tau)$ in a Taylor series about the point $\tau=0$ to get

$$F_{cl} = 2\pi \int_0^{\tau_{cl}} d\tau \left[f(0) + \sum_{n=1}^N \frac{1}{n!} f^{(n)}(0)\tau'^n \right] E_2(\tau_{cl} - \tau).$$

(22)

Completing the integration in Eq. (22) and then expanding the solution in a series about $\tau_{cl}=0$, one gets

$$F_{cl} = 2\tau_{cl}\sigma_{SB}T_{ds}^4 + O(\tau_{cl}^2).$$

(23)

Using this relation in Eq. (15) gives a second-order approximation to τ_{cl},

$$\tau_{cl} = \frac{T_f^4}{2T_{ds}^4}.$$

(24)

Therefore, the assumption that τ_{cl} is small depends on the final temperature being much less than the temperature just after the density jump. This value of τ_{cl} characterizes the emission in the cooling layer in an analogous fashion to characterizing a Gaussian by its peak value and width at half the peak value. Here the integral of the cooling layer emission times an E_2 function is characterized using the peak value of the emission, $2\sigma_{SB}T_{ds}^4$, times the width τ_{cl}.

The value of the thickness of the cooling layer is shown in Fig. 4. This thickness is less than 0.1 when Q is of the order of several thousand, a shock strength readily achieved in current experiments.[19,20]

Note that the relation in Eq. (24) could be used to compute the normalized upstream flux at the density jump F_{rn0} as a function of T_{dsn},

$$F_{rn0} = 4\tau_{cl}QT_{dsn}^4 + O(\tau_{cl}^2).$$

(25)

This, however, does not lead to an improved closed form solution for η_f and T_f to first order in τ_{cl} because τ_{cl} is a function of T_f and therefore also F_{rn0}.

E. Anomalous cooling

At this point it is also worth noting that the three-layer model allows final temperatures that are below the initial upstream temperature. This anomalous cooling phenomenon occurs in models of optically thin shocks where the so-called density collapse drives the final density to large values. Nevertheless, other authors[3,12] pointed out that some process not included in the model will force the final temperature to be no less than the initial temperature, and the same extra-model processes will place a lower limit on the final temperature as well. For instance, the material surrounding the shocked material might act as a temperature bath or magnetic field effects could limit the temperature increase.[3,12] The three-layer model assumes that there is no radiation absorption upstream of the density jump, so there is no precursor. If, on the other hand, the upstream medium has a very small but finite optical depth, and is initially cold so that it is heated by the radiation from the shocked material, then the ratio of precursor temperature to final temperature cannot greatly exceed unity.[3]

We do point out that it should not be surprising that a thick-thin radiating shock could be cooler downstream than upstream. To show this we appeal to the simplified description of the shock as a hot source radiating into a semi-infinite half space. In such a situation we can expect that there is a temperature at which radiation is the dominant mechanism for the shock to give up its energy due to the fact that the radiation flux scales as T^4. As the shock strength increases, the downstream temperature increases and, as a result, a greater fraction of the shock energy is radiated ahead of the density jump and, therefore, out of the system. This contrasts with the optically thick radiating shocks where radiation energy cannot leave the system.

As a result of the above analysis, there is a value of Q at which $RT_{fn}=RT_{0n}$. Such a situation could, somewhat imprecisely, be called an isothermal shock. Values of Q below this threshold value will have the $RT_{fn}>RT_{0n}$, and when Q is greater than the threshold, the final temperature will be below the initial temperature. Therefore, knowledge of which value of Q gives an isothermal shock will contain useful information about the character of the thick-thin radiative shock. Also, Drake used the isothermal shock case to derive several relations about the thick-thin shocks.[3] Here we will show under what conditions the shock is isothermal and derive several properties for this special case.

To find the value of Q that gives an isothermal shock, we will rewrite Eq. (12) with $RT_{fn}=RT_{0n}=p_{0n}$ and solve for F_{rn0} to get

$$F_{rn0} = 1 - p_{0n}^2,$$

(26)

under the restriction that $p_{0n} \leq \gamma$. Then substituting this value of F_{rn0} into Eq. (10) and solving for Q, one gets that the shock will be isothermal when

$$Q = \frac{1 - p_{0n}^2}{2p_{0n}^4}.$$

(27)

This value of Q can be written in terms of the traditional Mach number, $M^2=1/p_{0n}\gamma$, as
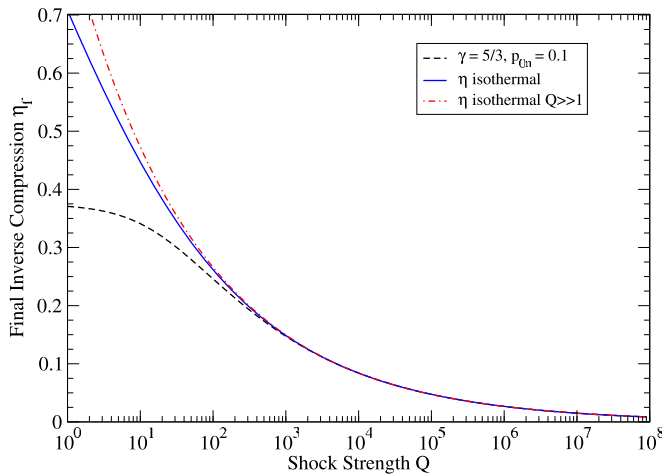
FIG. 5. (Color online) Values of the final inverse compression computed from the full three-layer model [i.e., Eq. (20)], the isothermal approximation [i.e., Eq. (29)], and the expansion of the isothermal approximation for large Q.

$$Q = \tfrac{1}{2}(M^8\gamma^4 - M^4\gamma^2). \tag{28}$$

This result has the proper limit; when $p_{n0}=0$, it takes an infinite shock strength to have zero temperature in the final state. Also, the isothermal shock strength might not be strong enough to make the cooling layer very optically thin. For example, with $p_{0n}=0.1$, the value of Q for an isothermal shock is 4950. For $\gamma=4/3$ at this shock strength, τ_{cl} is still larger than 0.1. Therefore, when $p_{0n}=0.1$ in a gas with $\gamma=4/3$, for the cooling layer to be negligibly small, the shock strength would have to be large enough to make the final temperature below the initial temperature.

The isothermal case also has $\eta_f=p_{0n}$, as can be found by substituting the value of F_{rn0} from Eq. (26) into Eq. (10) for $p_{0n} < \gamma$. Using this value of η_f in Eq. (27), one can solve for η_f in terms of the shock strength,

$$\eta_f = \sqrt{\frac{\sqrt{1+8Q}-1}{4Q}}. \tag{29}$$

This value for the final inverse compression can serve as a rule of thumb. If one assumes that the shock is isothermal, the final compression can be readily computed from the shock strength Q. The relation for the final inverse compression can be simplified by expanding Eq. (29) for large Q,

$$\eta_f = 0.840\,896 Q^{-1/4} + O(Q^{-3/4}). \tag{30}$$

The approximation for η_f given in Eq. (30) is remarkably accurate for $Q > 1000$ when compared with the solutions obtained from solving the quartic in Eq. (20). In Fig. 5 the inverse compression computed from the full three-layer model [i.e., Eq. (20)], the isothermal approximation [i.e., Eq. (29)], and the expansion of the isothermal approximation for large Q are compared. This figure shows that Eq. (30) is a useful rule of thumb for predicting the final inverse compression given the shock strength Q.
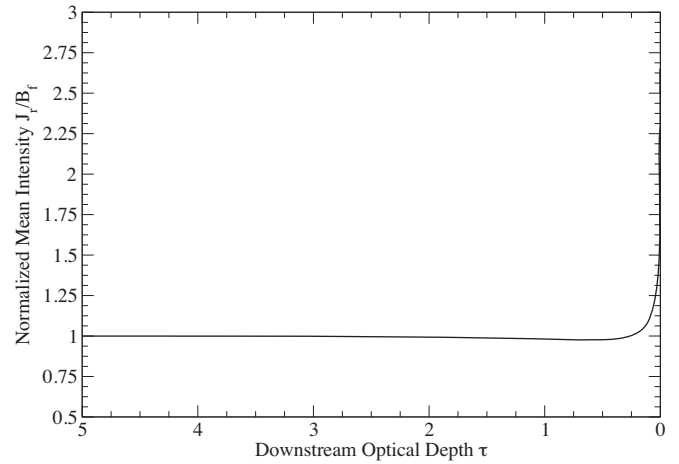
(a) J_r
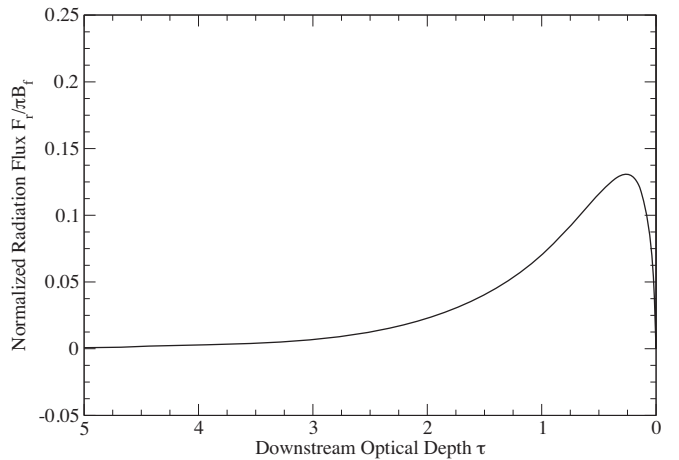
(b) F_r
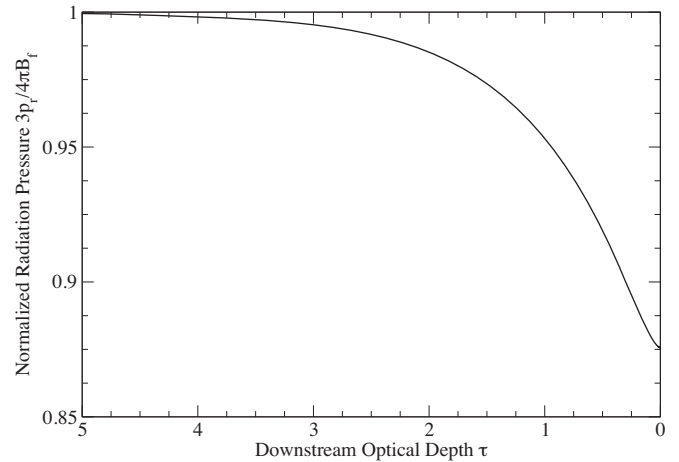
(c) p_r

FIG. 6. Normalized moments of the radiation intensity in the shocked material for a shock with $Q=10^5$, $\gamma=5/3$, and $p_{0n}=0.1$ as a function of downstream optical depth τ.

IV. RADIATIVE TRANSFER IN THE SHOCKED MATERIAL OF THE THREE-LAYER MODEL

In this section the properties of the radiation field downstream of the density jump in the three-layer model are investigated. For a more detailed discussion of radiative transfer in a hot, thin layer such as the cooling layer, the reader is
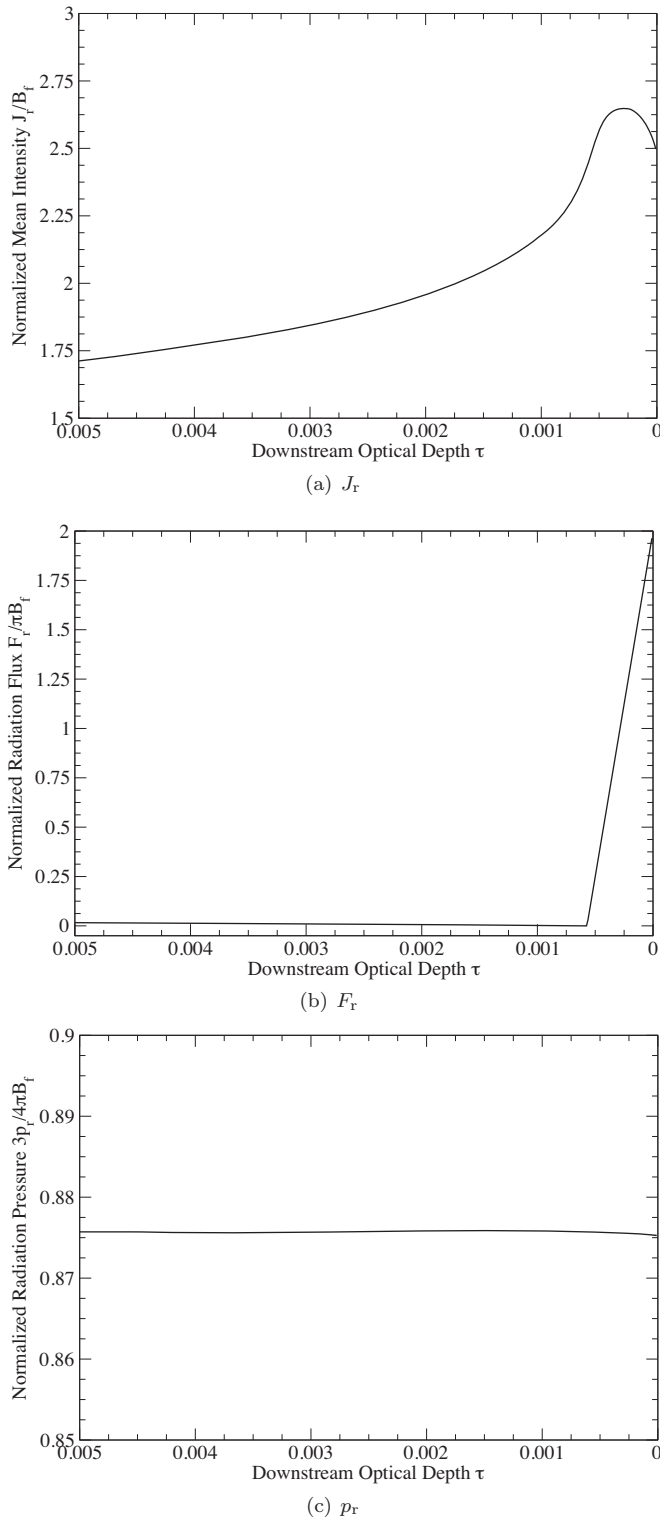
(a) J_r

(b) F_r

(c) p_r

FIG. 7. Detail of Fig. 6.

(a) Compression $(1/\eta)$

(b) T in units of u_s^2/R

FIG. 8. (Color online) Profiles of density and temperature for a shock with $\gamma = 5/3$, $p_{0n} = 0.1$, and $Q = 10^5$. The density jump is at $\tau = 0$ and $\tau > 1$ is downstream of the density jump.

$$2\sigma_{SB}T_{eff}^4[0.5 + E_3(\tau_{cl})] = 2\sigma_{SB}T_f^4. \qquad (31)$$

Using T_{eff} as the material temperature for $\tau \in [0, \tau_{cl}]$ and T_f as the temperature for $\tau > \tau_{cl}$, one can solve the integral transport equation to get the moments of the radiation intensity as a function of τ. In addition to the radiation flux F_r, one can compute the mean intensity J_r given by

$$J_r = \frac{1}{2}\int_{-1}^{1} I_r(\tau, \mu)d\mu,$$

and the radiation pressure p_r given by

$$p_r = \frac{1}{c}\int_{-1}^{1} \mu^2 I_r(\tau, \mu)d\mu.$$

Note the radiation energy density is related to the mean intensity by $E_r = 4\pi c J_r$.

In Figs. 6 and 7 these moments of I_r are plotted as a function of τ for a shock with $Q = 10^5$, $\gamma = 5/3$, and $p_{0n} = 0.1$. From Fig. 6 one sees that outside the cooling layer the mean intensity becomes equal to $B(T_f)$ and the value of the radiation pressure becomes equal to the radiation pressure of a blackbody at the final temperature. Inside and near

invited to consult Ref. 17. As a model for the material temperature in this region, the temperature in the cooling layer is approximated by a single temperature called T_{eff}, the effective temperature in the layer. To find T_{eff} one can solve for the temperature that produces a radiation flux that is equal and opposite to $2\sigma_{SB}T_f^4$ at the edge of the cooling layer,
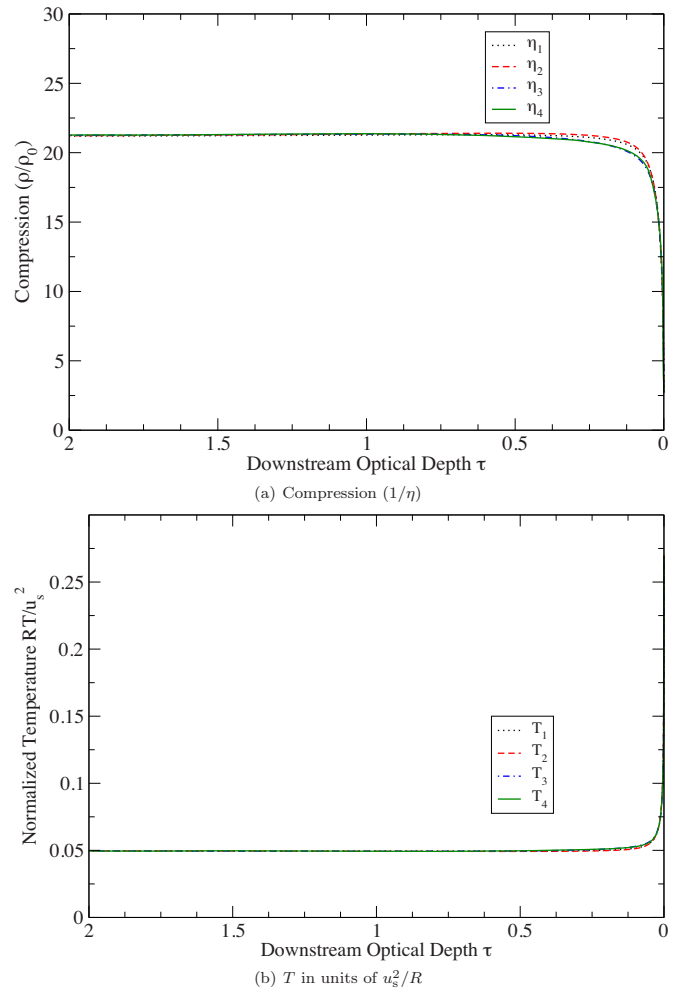
the cooling layer (see Fig. 7) the mean intensity reaches a maximum, whereas the radiation pressure is nearly flat. This is consistent with the picture of radiative transfer in a generic hot thin layer observed by McClarren and Drake.[17] These two quantities have different behavior because the intensity in the cooling layer has a very pancaked distribution: radiation traveling in the directions near $\mu=0$ has a higher intensity because of the $1/\mu$ weighting in the integral radiative transfer equation. This calculation of radiation pressure puts a much smaller weight on these angles than the mean intensity and it is radiation traveling at these grazing angles that causes the peak in the mean intensity. Inside the cooling layer the radiation flux falls linearly from $2\sigma_{SB}T_f^4$ to just below zero before rising to zero. Outside the cooling layer, the radiation flux rises to a value of 7.5% of its maximum within a mean-free path of the edge of the cooling layer. This rise can be attributed to a contribution to the radiation flux from the cooling layer persisting, while the radiation flux contribution from the final state decays to zero. As shown later, this rise is an artifact of neglecting the adaptation zone in the three-layer model. When the adaptation zone is included, this rise outside the cooling layer is smoothed out.

Note that radiative transfer behind the shock cannot be modeled, even qualitatively, with diffusion or a diffusive closure of the transport equation with a constant Eddington factor. This incompatibility of transport and diffusion can be seen by comparing J_r and F_r in the cooling layer. In the cooling layer there are places where the gradient of J_r is in the same direction as F_r. In the parlance of diffusion, at these points radiation is flowing uphill in an antidiffusive manner. Indeed the diffusion solution in the cooling layer does not have an extreme point and the peak in J_r is not present.[17]

V. SHOCK PROFILES

Now that the compression and temperature just after the density jump and at the final state have been calculated, as well as the thickness of the cooling layer, one is in a position to self-consistently compute the shock profile. The profile will be computed taking the adaptation zone into account as well as avoiding the assumption that the cooling layer is optically thin. This solution method begins with taking the spatial derivative of Eq. (9) to get an ordinary differential equation (ODE) for the inverse compression,

$$\frac{dF_{rn}}{d\tau} = \left[\frac{2\gamma(1+p_{0n})-2\eta(\gamma+1)}{\gamma-1} \right]\frac{d\eta}{d\tau}. \tag{32}$$

The left-hand side of the ODE can be simplified by integrating Eq. (2) over angle to get

$$\frac{dF_{rn}}{d\tau} = \frac{4\pi}{\frac{1}{2}\rho_0 u_s^3}[B(\tau)-J_r(\tau)]. \tag{33}$$

Therefore, if one has a profile for J_r it is possible to compute the profile for η from Eq. (32) (recall that B is function of T which is a function of η). The integration of the ODE is started at $\tau=0$, where $\eta=\eta_{ds}$.

One gets a profile for J_r using the simplified model of an effective temperature as computed in the previous section. This profile is used to solve the ODE for $\eta(\tau)$. This profile
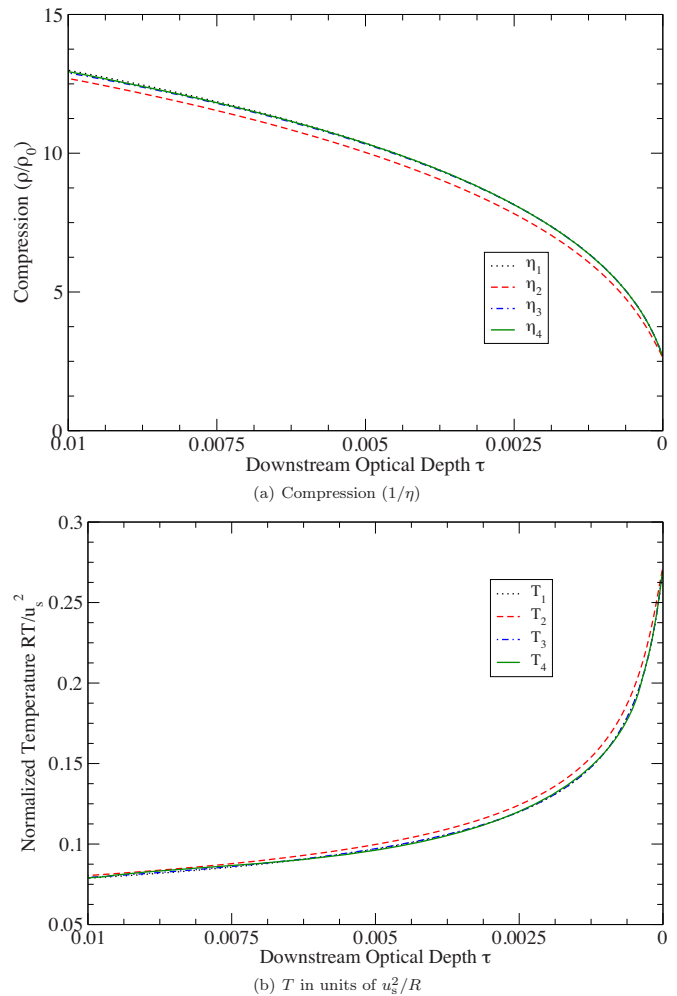
for η is called η_1 as it is the first in a series of iterations. Using η_1 one can compute a temperature profile T_1 to produce an iteration on the mean intensity, $J_{r,1}$. In these results it has been found that three such iterations of computing a profile for η and a new J_r are sufficient to converge on a profile.

This iterative procedure for computing a profile does take into account the adaptation zone between the cooling layer and the final state. This procedure makes no specification that the radiation flux goes to zero at the edge of the cooling layer. These results indicate that the effect of the adaption zone is small.

In Figs. 8–11 the profiles for the fundamental radiation and hydrodynamic quantities of a shock with $Q=10^5$, $\gamma=5/3$, and $p_{0n}=0.1$ are detailed. These figures include the profiles computed from each iteration of the solution procedure outlined above. There is little change in the temperature and compression profiles over the iterations. The radiation moments change more in the initial iterations but are converged by the third iteration. These profiles demonstrate that within one mean-free path of the density jump the shock has reached its final state. In these profiles, as seen in the three layer model, one observes that at points in the cooling layer $F_r/\nabla E_r>0$ and radiation energy is flowing uphill.

(a) Compression $(1/\eta)$

(b) T in units of u_s^2/R

FIG. 9. (Color online) Detail near density jump of Fig. 8.

(a) Normalized Mean Intensity $J_r/B(T_f)$

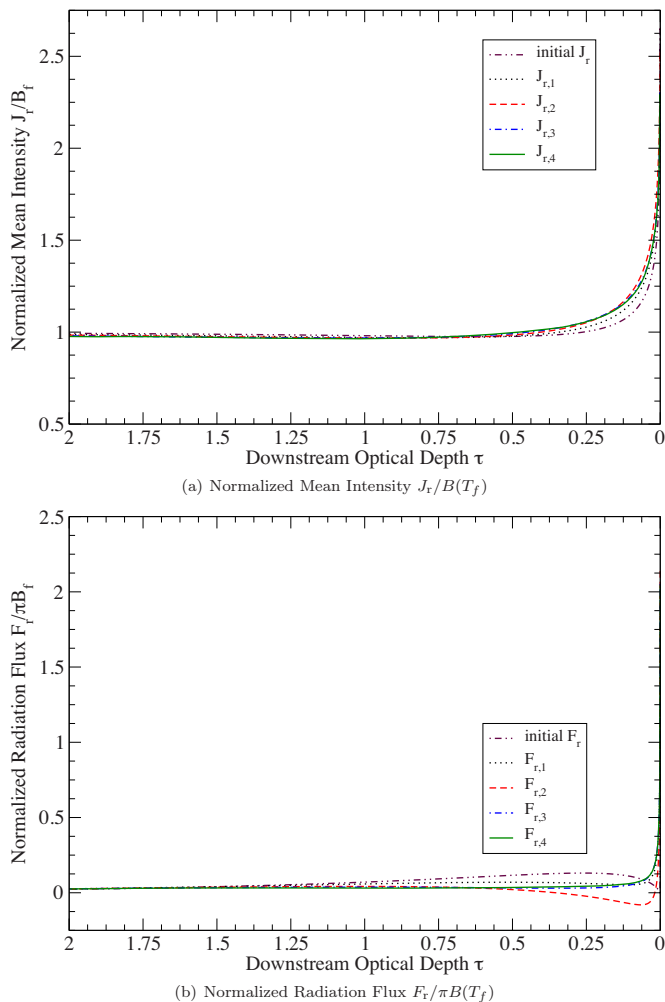(b) Normalized Radiation Flux $F_r/\pi B(T_f)$

FIG. 10. (Color online) Moments at different iterations of the radiation intensity for a shock with $\gamma=5/3$, $p_{0n}=0.1$, and $Q=10^5$. The density jump is at $\tau=0$ and $\tau>1$ is downstream of the density jump.

(a) Compression $(1/\eta)$

(b) T in units of u_s^2/R

FIG. 11. (Color online) Detail near density jump of Fig. 10.

Using the three-layer model, the final state has $\eta_f=0.0475$ (corresponding to a compression of approximately 21) and $RT_{fn}=0.05$ with $\tau_{cl}=0.000\,57$. These shock profiles confirm the predictions and validity of the three-layer model because the profiles include the adaptation zone and the emission in the cooling layer is not approximated using an effective temperature. It is also the case in these profiles that the upstream-moving radiation flux at the density jump is approximately $2\pi B(T_f)$ as argued above.

VI. CONCLUSIONS

The structures of radiative shocks that are optically thin upstream of the shock and optically thick downstream of the shock, which are referred to as thick-thin shocks, have been analyzed. This analysis dealt with the flux-dominated regime of shocks and viscous effects were ignored and it was assumed that the plasma could be characterized by a single temperature. To determine the shock structure, one has to deal with the fact that the radiation flux in the upstream region is implicitly dependent on the temperature at the final
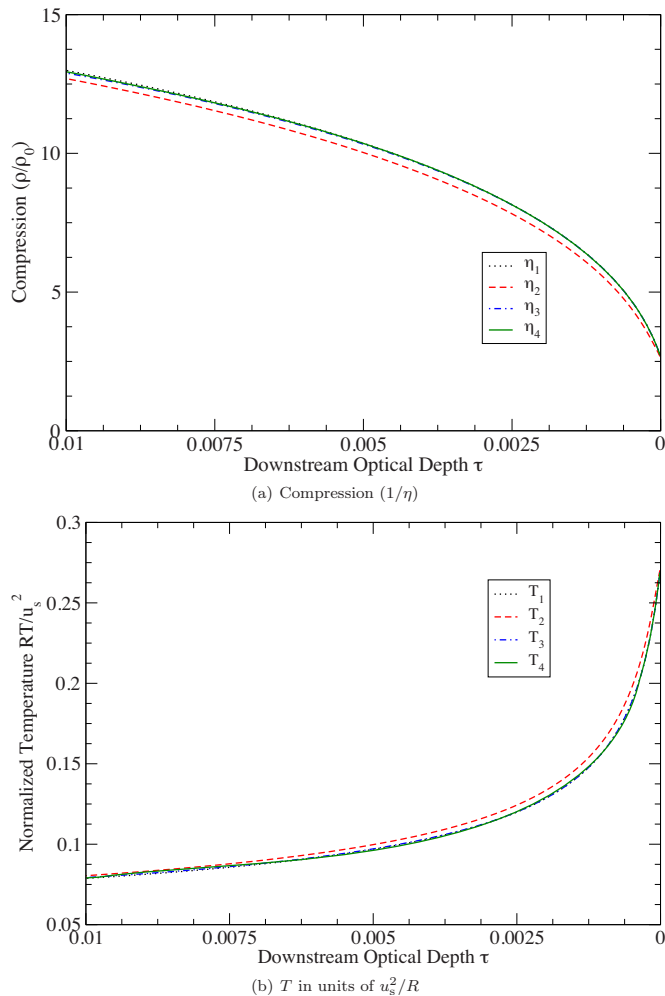
downstream state. Approximate radiative transfer treatments were not used to compute the downstream state of the system.

One of the salient features of thick-thin shocks is that the density just downstream of the density jump is greater than the maximum density in a radiative shock that is optically thick everywhere. For an infinite shock speed, the maximum density in a thick-thin shock is also infinite. Also, it was demonstrated that the radiation flux moving upstream from the density jump is, to leading order in the optical thickness of the cooling layer, twice the radiation flux emerging in the upstream direction from the final state. Later, it was confirmed that for sufficiently strong shocks the optical thickness of the cooling layer is indeed negligible. Also, as in the case of optically thin shocks, above a certain shock strength the three-layer model predicts a final temperature that is lower than the initial temperature and that the maximum compression in the shock scales as the shock strength to the 1/4 power.

Analyzing the radiative transfer in the shocked material revealed that there are points where the radiation flux is in the same direction as the gradient of the radiation energy density, i.e., radiation energy flows uphill. This is predicted by the three-layer model when the cooling layer emission is

approximated by a blackbody at an effective temperature and confirmed by calculations of shock profiles taking into account the adaptation zone. These shock profiles also confirmed the validity of the three-layer model. These profiles showed that the final state predicted by the three-layer model was accurate, yet that the transition from cooling layer to final state is more smoothed out than possible with a three-layer model.

The main deficiency of the above analysis is that no radiation from the upstream material returns to the shock structure. This is an assumption the authors plan to revisit in future work. Additionally, a comparison between theoretical results with numerical solutions and experiments is planned. Beyond these additional studies, one could augment this thick-thin shock model adding geometrical effects such as a radiating shock in a spherical object or the loss of radiation energy through the walls of a cylindrical tube from a shock propagating axially in a shock tube experiment.

ACKNOWLEDGMENTS

[1] Y. B. Zel'dovich and Y. P. Raizer, *Physics of Shock Waves and High-Temperature Hydrodynamic Phenomena* (Dover, Mineola, NY, 2002).

[2] D. Mihalas and B. Weibel-Mihalas, *Foundations of Radiation Hydrodynamics* (Dover, Mineola, NY, 1999).

[3] R. P. Drake, *High Energy Density Physics* (Springer-Verlag, New York, 2006).

[4] J. Castor, *Radiation Hydrodynamics* (Cambridge University Press, Cambridge, 2004).

[5] R. P. Drake, Phys. Plasmas **14**, 043301 (2007).

[6] R. P. Drake, IEEE Trans. Plasma Sci. **35**, 171 (2007).

[7] C. Michaut, E. Falize, C. Cavet, S. Bouquet, M. Koenig, T. Vinci, A. Reighard, and R. P. Drake, Astrophys. Space Sci. **322**, 77 (2009).

[8] R. P. Drake, Astrophys. Space Sci. **298**, 49 (2005).

[9] R. B. Lowrie and R. M. Rauenzahn, Shock Waves **16**, 445 (2007).

[10] R. B. Lowrie and J. D. Edwards, Shock Waves **18**, 129 (2008).

[11] R. A. Chevalier and J. N. Imamura, Astrophys. J. **261**, 543 (1982).

[12] F. H. Shu, *Gas Dynamics*, The Physics of Astrophysics Vol. II (University Science, Mill Valley, CA, 1992).

[13] K.-H. A. Winkler, M. L. Norman, and D. Mihalas, in *Multiple Time Scales*, edited by J. U. Brackbill and B. I. Cohen (Academic, San Diego, CA, 1985), p. 145.

[14] S. Bouquet, C. Stéhlé, M. Koenig J.-P. Chièze, A. Benuzzi-Mounaix, D. Batani, S. Leygnac, X. Fleury, H. Merdji, C. Michaut, F. Thais, N. Grandjouan, T. Hall, E. Henry, V. Malka, and J.-P. J. Lafon, Phys. Rev. Lett. **92**, 225001 (2004).

[15] M. Koenig, T. Vinci, A. Benuzzi-Mounaix, N. Ozaki, A. Ravasio, M. R. L. Glohaec, L. Boireau, C. Michaut, S. Bouquet, S. Atzeni, A. Schiavi, O. Peyrusse, and D. Batani, Phys. Plasmas **13**, 056504 (2006).

[16] M. González, C. Stéhlé, E. Audit, M. Busquet, B. Rus, F. Thais, O. Acef, P. Barroso, A. Bar-Shalom, D. Bauduin, M. Kozlova, T. Lery, A. Madouri, T. Mocek, and J. Polan, Laser Part. Beams **24**, 535 (2006).

[17] R. G. McClarren and R. P. Drake, J. Quant. Spectrosc. Radiat. Transf. **111**, 2095 (2010).

[18] R. B. Lowrie, J. E. Morel, and J. A. Hittinger, Astrophys. J. **521**, 432 (1999).

[19] A. B. Reighard, R. P. Drake, K. K. Dannenberg, D. J. Kremer, E. C. Harding, D. R. Leibrandt, S. G. Glendinning, T. S. Perry, B. A. Remington, J. Greenough, J. Knauer, T. Boehly, S. Bouquet, L. Boireau, M. Koenig, and T. Vinci, Phys. Plasmas **13**, 082901 (2006).

[20] F. W. Doss, H. F. Robey, R. P. Drake, and C. C. Kuranz, Phys. Plasmas **16**, 112705 (2009).